analytical chemistry

Editors' Highlight

pubs.acs.org/ac

Profiling Deacetylase Activities in Cell Lysates with Peptide Arrays and SAMDI Mass Spectrometry

Hsin-Yu Kuo,[†,∥] Teresa A. DeLuca,[‡,∥] William M. Miller,*[,‡,§] and Milan Mrksich*[,†,§]

[†]Departments of Biomedical Engineering, Chemistry, and Cell and Molecular Biology and [‡]Chemical and Biological Engineering, Northwestern University, Evanston, Illinois, 60208 United States

[§]Robert H. Lurie Comprehensive Cancer Center of Northwestern University, Chicago, Illinois, 60611 United States

Supporting Information

ABSTRACT: The development of arrays that can profile molecular activities in cells is important to understanding signaling pathways in normal and pathological settings. While oligonucleotide arrays are now routinely used to profile global gene expression, there is still a lack of tools for profiling enzyme activities in cell lysates. This paper describes the combination of peptide arrays formed on self-assembled monolayers and mass spectrometry to provide a label-free approach for identifying patterns of enzyme activities in cell lysates. The approach is demonstrated by profiling lysine deacetylase (KDAC) activities in cell lysates of the CHRF megakaryocytic (Mk) cell line. Class-specific deacetylase inhibitors were used to show that terminal Mk differentiation of CHRF cells is marked by a pronounced decrease in sirtuin activity and by little change in activity of KDACs 1-11. This work establishes a platform that can be used to identify changes in global activity profiles of cell lysates for a wide variety of enzymatic activities.

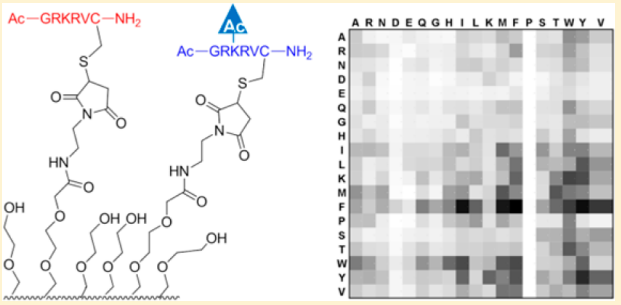

Different cell types, including differentiated states or pathological phenotypes, are characterized by unique patterns of gene expression and protein activities. While it is now routine to profile the former, there is still a lack of tools to profile large numbers of enzyme activities in cell lysates or other complex samples. Such tools are needed because changes in enzyme activities are often regulated at a post-transcriptional level and because they can provide a more direct understanding of the pathways that operate in cells. Endogenous activities in lysates are routinely assayed using fluorogenic reagents; however, the labels can alter the activity,[1] and the assays are difficult to scale to the parallel analysis of hundreds or thousands of activities. Peptide arrays offer opportunities to profile activities more broadly, and important early work has focused on understanding substrate specificities of enzymes but to a lesser extent for profiling lysates for activities of a protein family.[2] This paper describes a method to use peptide arrays and label-free analysis to profile lysine deacetylase enzyme activities in lysates at different stages of cell differentiation.

The acetylation of lysine side chains is now recognized to be a widespread post-translational modification that regulates protein function in a variety of signaling contexts.[3] Protein acetylation is regulated by twenty lysine acetyl transferase enzymes that use acetyl-CoA as a cofactor to install the acetyl group and by seventeen lysine deacetylases (KDACs) that remove this modification. The KDACs include six NAD^+-dependent sirtuins (SIRTs) and eleven divalent ion-dependent deacetylases (KDACs 1-11). How the specificities of these thirty-seven enzymes are coordinated to allow regulation of the acetylation states of thousands of protein substrates is a complex question and remains largely unexplored. The enzymes are most commonly assayed using a fluorescent "Fluor de Lys" (FdL) assay wherein peptide substrates are conjugated to a coumarin group, such that deacetylation of the peptide is then followed by proteolysis with release and detection of the coumarin group. The FdL reagents, however, are limited in their ability to resolve activities of the individual deacetylases and are known to report activities that are artifacts of using the fluorescently labeled reagents.[1]

The current work uses a label-free assay that overcomes these limitations (Figure 1). The "SAMDI" assay employs peptide substrates containing an acetylated lysine residue and also a terminal cysteine residue.[4] The peptide is added to a cell lysate, where it can be deacetylated by endogenous enzymes in the lysate. The reaction is then quenched by the addition of deacetylase inhibitors and applied to a self-assembled monolayer having maleimide groups at a density of 25% against a background of tri(ethylene glycol) groups. The peptide substrate undergoes immobilization, in both its acetylated and deacetylated forms, to the monolayer by reaction of the terminal cysteine residue with the maleimide group. The tri(ethylene glycol) groups are effective at preventing nonspecific adsorption of proteins and other lysate components to the monolayer. The monolayer can then be

Received: August 16, 2013
Accepted: October 2, 2013
Published: October 2, 2013

   dx.doi.org/10.1021/ac402614x | Anal. Chem. 2013, 85, 10635−10642

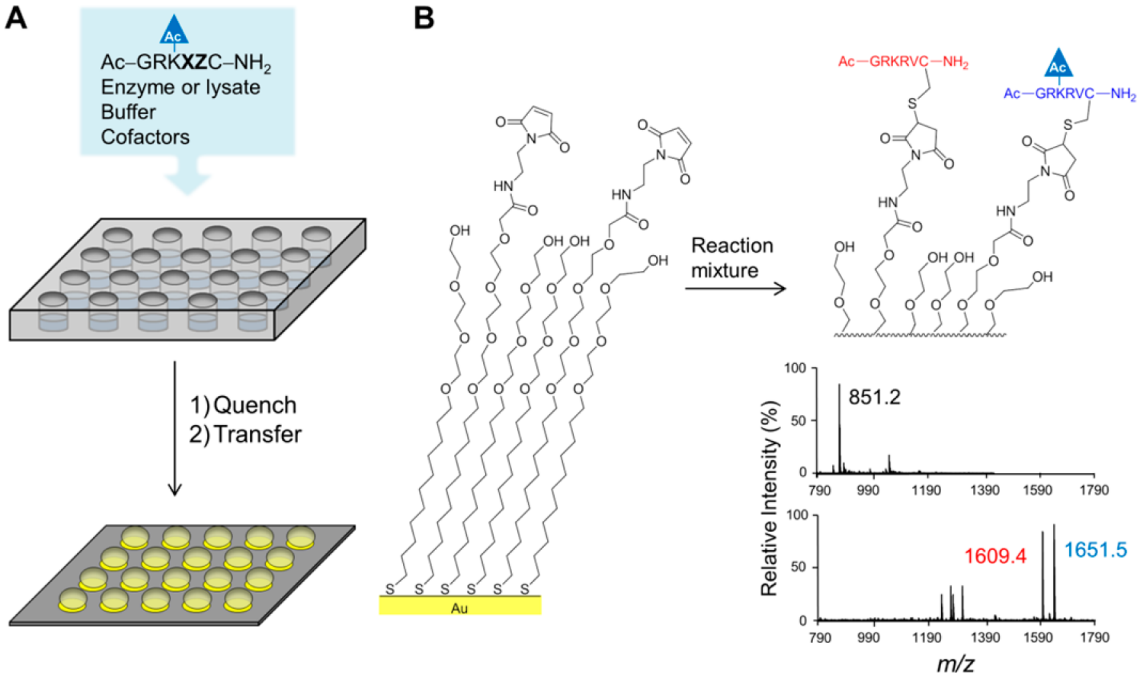

Figure 1. SAMDI assay for profiling deacetylase activities. (A) Cysteine-terminated peptides containing an acetylated lysine are individually incubated with a cell lysate in wells of a plate. The reactions are then quenched and transferred to a plate containing gold islands with a monolayer presenting maleimide groups. (B) The cysteine-terminated peptides, in both the acetylated and deacetylated forms, immobilize to the monolayer and are analyzed by MALDI mass spectrometry. The SAMDI spectra show the presence of the maleimide-terminated alkanethiol prior to peptide immobilization (top spectrum, at m/z 851) and after immobilization of a reaction mixture to identify peaks for the immobilized peptide substrate (bottom spectrum, m/z 1651) and its deacetylated form (m/z 1609). The peak areas for the acetylated and deacetylated forms of the peptide are integrated to calculate the percent conversion for the deacetylation.

analyzed by matrix-assisted laser desorption-ionization (MALDI) mass spectrometry to identify the masses of the peptide−alkanethiolate conjugates and to quantitate the fraction of the peptide that has been deacetylated by endogenous enzymes in the lysate (Figure 1). In the present paper, we demonstrate the use of arrays comprising hundreds of peptide substrates to directly profile deacetylase activities in the CHRF megakaryocytic (Mk) cell line, and we show that terminal Mk differentiation of the CHRF cells leads to a profound decrease in sirtuin activities.

EXPERIMENTAL SECTION

Reagents. All reagents were obtained from Sigma-Aldrich, except as indicated below. EX-527 was obtained from Cayman Chemical. Trichostatin A (TSA) was obtained from Santa Cruz. Phorbol-12-myristate-13-acetate (PMA) was obtained from Calbiochem.

Preparation of Cell Lysate. Cell lysates were prepared on the basis of a protocol adapted from previous reports.[2d,5] Cells were washed once with phosphate-buffered saline (PBS), and the cell pellet was frozen at −80 °C. The remaining steps were performed on ice or at 4 °C. The cell pellet was resuspended in Buffer E (20 mM 4-(2-hydroxyethyl)-1-piperazineethanesulfonic acid (HEPES, pH 7.9), 5 mM potassium acetate, 0.5 mM $MgCl_2$, 0.5 mM dithiothreitol (DTT), 0.1 mM phenylmethylsulfonyl fluoride (PMSF)) and incubated on ice for 10 min. A Dounce homogenizer with loose pestle was used to disrupt cells with 25 strokes. The extract was then spun at 1500g for 3 min to pellet the nuclei (and cell debris). Nuclei were resuspended in Buffer N (Buffer E + 0.6 M NaCl) and incubated for 90 min with gentle shaking. The cytosolic and nuclear extracts were spun at 14 000g for 20 min, and the supernatant extracts were combined to achieve a whole cell extract. This whole cell lysate was dialyzed against Buffer D (20 mM HEPES (pH 7.9), 20% glycerol, 0.1 M KCl, 0.2 mM EDTA, 0.5 mM Tris(2-carboxyethyl)phosphine (TCEP), 0.1 mM PMSF) and then stored at −80 °C. Protein concentration was measured using the BCA protein assay (Thermo Scientific/Pierce).

Deacetylase Activity Assay in Lysates. Cell extracts were diluted in KDAC buffer (25 mM Tris (pH 8.0), 137 mM NaCl, 2.7 mM KCl, 1 mM $MgCl_2$) to a final protein concentration of 1 mg/mL. For total deacetylase activity measurement, no inhibitors were added; for measuring sirtuin activity, TSA was added to diluted cell extracts to give a final concentration of 50 μM; for KDAC 1-11 activity, nicotinamide (NIC) was added at a final concentration of 50 mM. Next, 5 μL of the resulting mixtures was distributed into separate wells of a 384-well plate. A protease inhibitor cocktail (1 μL, Roche) and NAD^+ (1 μL, 1 mM final) were added to each reaction well. To initiate the reaction, 1 μL of the acetylated peptide substrates was added at a final concentration of 10 μM. The reaction plate was incubated at 37 °C for 1 h and quenched with the deacetylase inhibitors Trichostatin A (TSA, 50 μM) and nicotinamide (NIC, 50 mM).

Mass Spectrometry. Small volumes of each reaction (2 μL) were transferred onto an array plate having 384 gold islands modified with a maleimide-presenting monolayer to allow immobilization of the peptide substrate and product. The monolayers were then rinsed with deionized ultrafiltered (DIUF) water and ethanol, dried under nitrogen, and treated with matrix (2,4,6-trihydroxyacetophenone, 20 mg/mL in acetone). The monolayers were analyzed by MALDI-TOF MS to obtain a mass spectrum for each spot. Mass analysis was

dx.doi.org/10.1021/ac402614x | Anal. Chem. 2013, 85, 10635−10642

performed using a 4800 MALDI-TOF/TOF mass spectrometer (Applied Biosystems). A 355 nm Nd:YAG laser was used as a desorption/ionization source, and all spectra were acquired with 20 kV accelerating voltage using positive reflector mode. The extraction delay was 450 ns; 3000 laser shots were applied, and the entire surface of the gold spot was sampled. Activities were calculated from each spectrum as previously described.[2d]

Solid Phase Peptide Synthesis. Lanterns (Mimotopes) were placed in each well of a 96-well filter plate with filters plugged. The N-terminal fluorenylmethyloxycarbonyl (FMOC) was deprotected with 20% piperidine in *N*,*N*-dimethylformamide (DMF) for 10 min; the solvent was then filtered with a vacuum manifold. The lanterns were then washed 5 times with DMF. A solution containing 15 equivalents of amino acid, hydroxybenzotriazole (HOBt), and diisopropylcarbodiimide (DIC) was prepared, applied to each well, and incubated at RT for 2 h. The solutions were then filtered; the lanterns were washed 5 times with DMF, and then, the process was repeated. After the last step of coupling, a cleavage cocktail was applied to the lanterns containing 95% trifluoroacetic acid (TFA), 2.5% H_2O, and 2.5% triethylsilane (TES), and the lanterns were incubated at RT for 2 h. The solutions were then evaporated by flowing nitrogen over the plate for 16 h. The residues were taken up in water, transferred to a 96-well plate, and lyophilized overnight. The remaining solids were then suspended in DIUF water with 0.1% TFA and stored in a 384-well plate at −20 °C.

Cell Culture. The CHRF-288-11 cells were cultured in Iscove's Modified Dulbecco's Medium (IMDM) plus 10% fetal bovine serum (FBS) in a humidified chamber at 37 °C, 5% CO_2. On day 0, the basal cells were seeded at 100 000/mL in tissue culture flasks and stimulated with 10 ng/mL PMA (Calbiochem). At the time points indicated, trypsin-EDTA was used to collect the adherent cells for analysis.

Flow Cytometry. For ploidy analysis, cells were washed, fixed in 0.5% paraformaldehyde for 15 min at room temperature, permeabilized with 70% cold methanol, and treated with RNase for 30 min at 37 °C, and DNA was stained with propidium iodide. Samples were acquired on an LSRII flow cytometer with FACSDiva software (BD Biosciences).

Western Blots. Cell lysates from the array experiments were used for the Western blots. Protein was denatured, separated by Mini-PROTEAN TGX Precast Gels (BioRad), and transferred onto nitrocellulose membranes (BioRad). The membranes were blocked with 5% nonfat dry milk or 5% bovine serum albumin (BSA) in Tris-buffered saline +0.1% Tween 20 (TBST) buffer for 1 h. Membranes were incubated with primary antibody in TBST + 5% milk or BSA with gentle shaking for 2 h at room temperature or overnight at 4 °C. Membranes were washed and incubated with horseradish peroxidase (HRP)-conjugated antimouse or antirabbit-IgG antibody (Cell Signaling). Protein was detected using Chemiluminescent HRP Substrate (Millipore) and film exposure. Membranes were washed in TBST and stripped (62.5 mM Tris-HCl (pH 6.7), 2% sodium dodecyl sulfate (SDS), 100 mM beta-mercaptoethanol) for 30 min at 50 °C. Membranes were washed with TBST, and then, the entire procedure was repeated for detection of beta-actin. Densitometry was done using ImageJ software.[6] The SIRT1 (#32424) and beta-actin (#8226) antibodies were obtained from Abcam; SIRT2 (#04−1124) and SIRT5 (#ABE198) from Millipore; SIRT3 (#5490) and SIRT6 (#2590) from Cell Signaling; SIRT7 (sc-135055) from Santa Cruz.

RESULTS

KDAC Activity in CHRF Cell Cultures. We measured deacetylase activities in lysates prepared from the CHRF-288-11 megakaryocytic cell line. Basal CHRF cells exhibit an immature Mk phenotype but respond to the phorbol ester PMA (phorbol-12-myristate-13-acetate) by displaying phenotypic and morphological changes characteristic of Mk maturation.[7] The cells undergo endomitosis (DNA replication without cytokinesis) resulting in increased ploidy and, as part of terminal maturation, the cells extend cytoplasmic protrusions known as proplatelets (Figure 2).

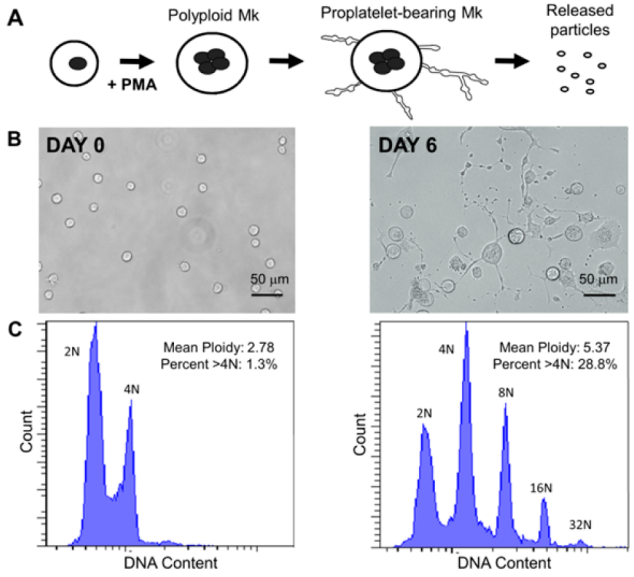

Figure 2. (A) Treatment of CHRF cells with PMA (phorbol-12-myristate-13-acetate) stimulates a differentiation process that results in polyploidization and extension of proplatelets. (B) Light microscope images of CHRF cells before (day 0) and after (day 6) treatment with PMA. (C) Ploidy histograms of CHRF cell cultures illustrate the polyploidization of differentiating cells.

We first used eight peptides, which were identified as substrates for human deacetylases in earlier work[2d,8] and are listed in Table S1, Supporting Information, to measure deacetylase activities in lysates of unstimulated CHRF cells. The cell lysate was distributed in the wells of a 384-well microtiter plate with 1 mM NAD^+ (Figure S1, Supporting Information) in KDAC buffer, followed by the addition of a peptide substrate to each well at 10 μM. The reactions were allowed to proceed for 60 min and then quenched with the deacetylase inhibitors trichostatin A (TSA, 50 μM) and nicotinamide (NIC, 50 mM) (Figure S2, Supporting Information) and transferred to an array plate having 384 gold islands using a Tecan EVO liquid handler. The islands were modified with a monolayer presenting maleimide groups against a background of tri(ethylene glycol) groups and therefore allowed immobilization of the cysteine-terminated peptides. We confirmed that the peptides, in both the acetylated and deacetylated forms, underwent immobilization at a comparable rate. After 60 min, the array plates were rinsed with deionized ultrafiltered water, followed by ethanol, and then treated with matrix (2,4,6-trihydroxyacetophenone, 20 mg/mL in acetone) and analyzed by SAMDI mass spectrometry. Yields for deacetylation of each peptide were determined by taking the ratio of the peak area for the deacetylated peptide

to the sum of the peak areas for the substrate and product peptides (Figure 3, blue bars). The peptides undergo

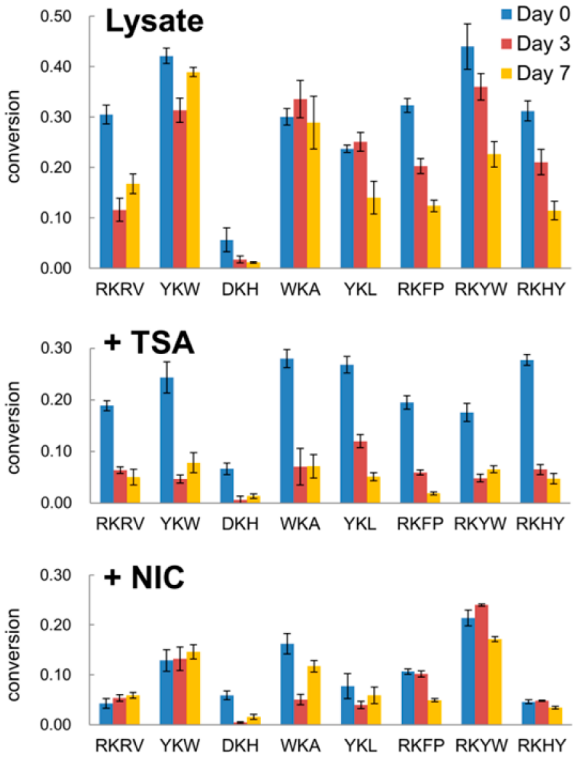

Figure 3. The extent of deacetylation is shown for each of eight peptides treated with CHRF cell lysates before treatment (day 0, blue) and at 3 days (red) and 7 days (yellow) after treatment with PMA. Experiments were also performed with lysates supplemented with TSA to observe SIRT activity and with NIC to observe KDAC 1-11 activity. Each experiment was performed in four replicates, and error bars represent the standard deviation.

deacetylation to different extents, reflecting their different activities toward the endogenous deacetylases. For example, the DKH peptide shows 5% deacetylation, and the RKYW peptide shows 44% deacetylation. We also used pan-specific inhibitors to partially resolve the deacetylase activities. Supplementing the lysates with TSA, for example, inhibits KDACs 1-11[9] and therefore can reveal the fraction of deacetylase activity attributed to the sirtuins (Figure S3A, Supporting Information). Similarly, treatment of the lysates with NIC inhibits the sirtuins[10] and therefore reveals the activities derived from KDACs 1-11 (Figure S3B, Supporting Information). The two activities in these inhibited lysates generally sum to give the activity observed in the untreated lysate. For example, the RKHY peptide undergoes 31% deacetylation in untreated lysate, but reacts at 27% in TSA-treated lysate and 4% in NIC-treated lysate (Figure 3).

We also treated CHRF cells with PMA to induce differentiation, and we prepared and tested lysates isolated after three (Figure 3 red bars) and seven days (Figure 3 yellow bars) in culture. Several peptides reveal that the deacetylase activities decreased as differentiation proceeded. For example, the extent of deacetylation for the RKRV, YKL, RKFP, RKYW, and RKHY peptides decreased by 2- or more fold over one week in culture. Further, characterization of lysates treated with inhibitor showed that these changes resulted primarily from a decrease in sirtuin activity and not the activities of KDACs 1-11. That is, TSA-treated lysates showed a decrease in deacetylation over the course of differentiation whereas NIC-treated lysates showed less significant changes.

Protease Interference. When first performing these experiments, we found that several of the spectra did not give the expected peaks for the acetylated and deacetylated forms of the peptide. Rather, we observed peaks corresponding to truncated forms of the peptide, and we recognized that endogenous proteases were digesting the substrates. For example, the expected peak in the mass spectrum for the GRK^{Ac}RVC peptide was almost absent relative to new peaks associated with cleavage of the peptide at the valine and arginine residues. We evaluated common protease inhibitor cocktails to control this unwanted reaction and found that addition of the Roche EDTA-free protease inhibitor cocktail blocked much of the proteolysis without affecting deacetylase activity (Figures 4 and S4, Supporting Information). With

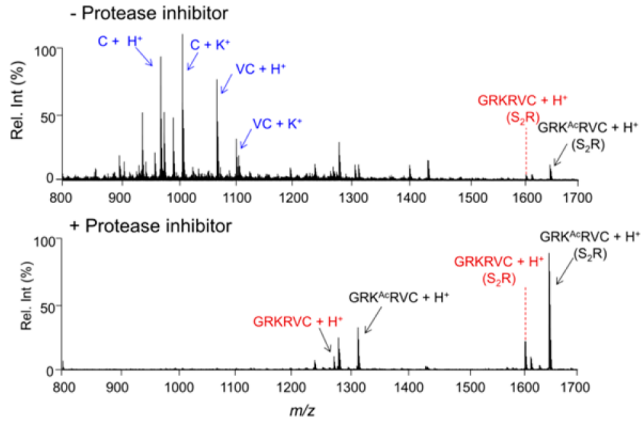

Figure 4. SAMDI revealed that the peptides were degraded by proteases in the lysate. A SAMDI spectrum of a monolayer to which the peptide GRK^{Ac}RVC was immobilized after treatment with lysate revealed several peaks (in blue) attributed to proteolysis (top spectrum). The use of a protease inhibitor cocktail in the assay blocked this degradation and allowed observation of the peptide in its acetylated (black) and deacetylated form (red, bottom spectrum). The SAMDI spectrum reveals peaks for alkanethiolates and for the corresponding dialkyl disulfide forms of the molecule (R^1SSR^2). The major products observed when protease activity was present corresponded to products resulting from proteolytic cleavages at the C-terminus of arginine and at the C-terminus of valine (Figure S4, Supporting Information).

many label-dependent assays, only the products of the biochemical reactions are observed and a lack of product is interpreted as a lack of activity in the sample. The use of SAMDI, however, reveals the composition of the monolayer in each assay spot and, in this case, immediately revealed that proteases were cleaving peptide fragments from the substrate so that they were not available for recording deacetylase activities.

Peptide Arrays. Our initial experiments with CHRF cell lysates showed that the SAMDI assay could measure deacetylase activities in cell lysates and that these activities could be resolved into the two subclasses. However, the use of eight peptides, while providing greater resolution than the existing assays based on fluorogenic reagents, was insufficient to provide activity profiles that might be used to identify roles for protein acetylation in regulating cellular programs. Hence, we moved to arrays containing 361 peptides to assay the lysates. The peptides had the sequence Ac-GRK^{Ac}**XZ**C-NH$_2$, where

dx.doi.org/10.1021/ac402614x | *Anal. Chem.* 2013, 85, 10635−10642

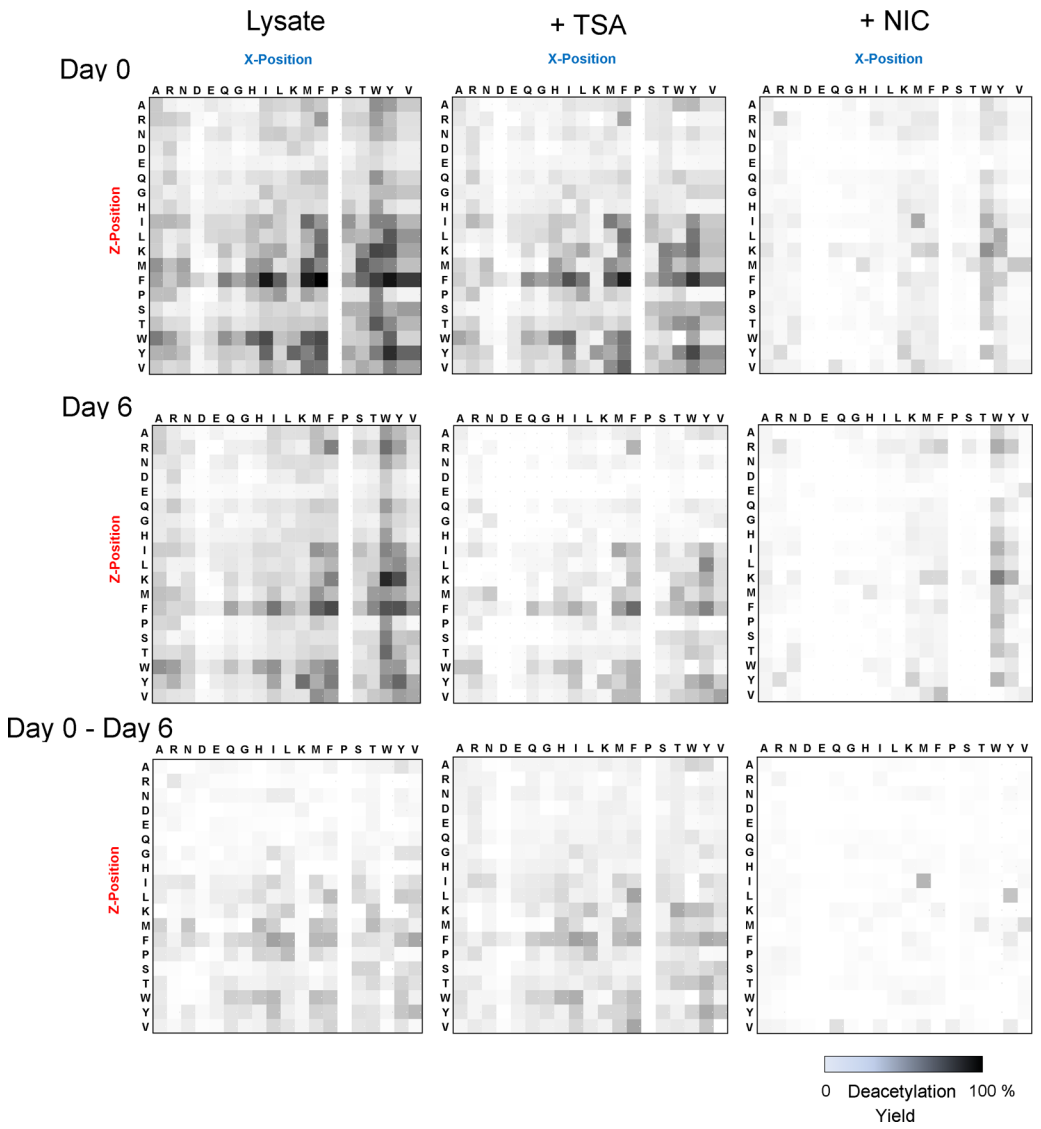

Figure 5. Heatmaps showing the extent of deacetylation of each peptide after treatment with lysate. A library of 361 peptides of the sequence Ac-GRK^{Ac}**XZ**C-NH_2, where individual peptides had unique combinations of nineteen amino acids (all except cysteine) at the X and Z positions, was treated with lysate, immobilized, and analyzed by SAMDI to determine the extent of deacetylation, which is shown in gray scale. Lysates were probed before (day 0) and 6 days after treatment with PMA. The lysates were also tested after supplementation with TSA or NIC to observe SIRT or KDAC 1-11 activities, respectively. The bottom row has difference heatmaps which were determined by subtracting the conversion for day 6 from that at day 0 to reveal changes in the patterns of activity.

individual peptides had unique combinations of nineteen amino acids (all except cysteine) at the X and Z positions. We again distributed cofactors, buffer, and lysates prepared from CHRF cells in the wells of a 384-well microtiter plate. Individual peptides were added to the lysates, and the reactions were allowed to proceed for 60 min and then were quenched with deacetylase inhibitors and robotically transferred to an array plate that had 384 gold islands each having a monolayer as described above. The plates were incubated for 60 min to allow immobilization of the peptides and were then analyzed by SAMDI mass spectrometry. Representative SAMDI spectra are shown in Figure S5, Supporting Information. Peak areas were integrated to determine the percent conversion of each peptide to its deacetylated form, and these conversions were plotted in the form of a heat map to give a deacetylase activity profile for each lysate (Figure 5 and Data Set S1).

We analyzed lysates prepared from untreated cells and from cells 6 days after treatment with PMA. We also analyzed lysates that were treated with either TSA or NIC. The array data are presented in the form of a heatmap that uses a grayscale to indicate the extent of deacetylation observed for each peptide. The heatmap for the unstimulated (day 0) lysate shows that the peptides spanned a range of activities, with 85 of them showing more than 30% deacetylation, 219 showing from 5% to 30% deacetylation, and 57 showing little or no deacetylation. Further, the heatmaps for the TSA- and NIC-treated lysates prepared from unstimulated cells (day 0) show that the majority of the deacetylase activities can be ascribed to the sirtuins; that is, the activities are inhibited by NIC but not TSA. We also found that lysates prepared from cells 6 days following PMA treatment (day 6) were characterized by a marked loss of deacetylase activities and that this loss was largely due to a decrease in sirtuin activities. For example, the heatmaps for the TSA-treated lysates show less activity at day 6 relative to day 0, whereas the heatmaps for the NIC-treated lysates are largely

dx.doi.org/10.1021/ac402614x | *Anal. Chem.* 2013, 85, 10635−10642

similar. This result is consistent with our findings using the small panel of 8 peptides (Figure 3).

To gain additional insight into which sirtuins were responsible for the decrease in deacetylase activity, we analyzed the lysates by Western blotting for each of the six enzymes (Figure 6A). These blots show that SIRTs 1 and 2 are present

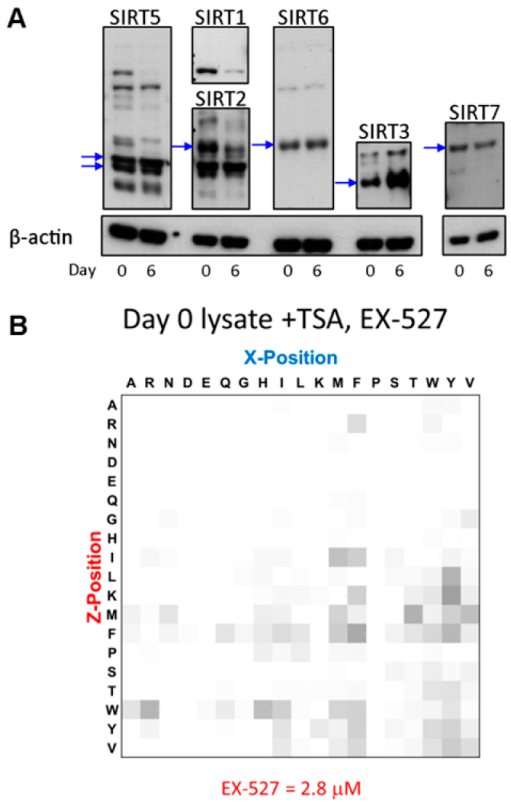

Figure 6. (A) Western blots for the SIRT deacetylases in CHRF cells before (day 0) and after (day 6) PMA stimulation (protein bands are indicated by the blue arrows). Densitometry quantification is shown in Figure S6, Supporting Information. (B) Heatmap for lysates supplemented with TSA and the SIRT 1/2 antagonist EX-527. Inhibition of SIRTs 1 and 2 in lysates of unstimulated cells gave a heatmap that is similar to that for lysates from day 6 of PMA-stimulated cells. The cosine similarity for the two vectorized activity profiles is 0.83 (r = 0.83). Actin is shown to calibrate protein loading in the gel.

at lower levels, while SIRT3 is present at a higher level, in the differentiated cells. The small molecule EX-527 has been reported as a selective inhibitor for SIRT1 and to a lesser extent of SIRT2,[11] and we therefore used this inhibitor to address whether the loss in sirtuin function evident in the heatmaps at days 0 and 6 could be explained by a decrease in the activities of these two enzymes. We added EX-527 at a concentration of 2.8 μM to the TSA-treated lysate from day 0 and analyzed this lysate on the peptide array (Figure 6B). The heatmap for the latter condition, where SIRT1 is largely inhibited, SIRT2 is partially inhibited, and SIRT3 is essentially uninhibited, was very similar to the heatmap observed for TSA-treated lysates at day 6 (cosine similarity is 0.83). That is, the difference in sirtuin activities at days 0 and 6 was consistent with loss of SIRT1 and SIRT2 activity. Again, these experiments reveal how peptide arrays, in combination with selective inhibitors, can be used to profile enzyme activities in lysates and to identify those enzymes that are modulating the activity profiles.

DISCUSSION

This work demonstrates that the combination of peptide arrays prepared on self-assembled monolayers of alkanethiolates on gold and MALDI mass spectrometry is effective at measuring endogenous enzyme activities in complex cell lysates. There have been several important reports of methods for the global profiling of biochemical activities.[2a−c,12] Most significant is the SPOT technology that prepares peptide arrays on nitrocellulose paper.[2a−c] These arrays have been valuable in profiling enzyme specificity in biochemical experiments but are less effective in analyzing complex samples, in part because of protein adsorption to the array and because they are not compatible with many analytical methods, including surface plasmon resonance spectroscopy and mass spectrometry. The monolayers address these limitations by offering a well-defined surface chemistry that controls unwanted protein adsorption, maintains a uniform density of ligand across the array, and is compatible with a broad range of immobilization chemistries. The use of monolayers is also uniquely suited for analysis by mass spectrometry, and previous work has shown that the SAMDI method is quantitative and has good reproducibility across the array plate.[13]

Our work used a collection of small peptides to measure deacetylase activities, even though the peptides are not mimics of cellular substrates for these enzymes. However, what is important is that the peptides display a range of activities toward the deacetylases and that they can resolve the activities of members of the enzyme family. The peptides are diverse in the functional groups proximal to the acetylated lysine residue and therefore have different affinities for the enzyme active sites. It is these differences that allow the peptides to have differential activities toward the individual enzymes. The resulting pattern of activities that is observed on the array provides a fingerprint characteristic of the set of enzymes that are active in the lysate, and for this reason, the arrays can be used to monitor differences in enzyme activities between two cell cultures. In this sense, the arrays are primarily suited to profile lysates for global deacetylation activity, rather than to identify the specific enzymes that are present in the sample.

This work also provides the first example of using peptide arrays to profile endogenous deacetylase activity in cellular lysates. While the Fluor de Lys fluorogenic reagents can be used to monitor deacetylase activities in lysates,[14] the limited number of available reagents makes it difficult to obtain profiles of deacetylase activity. Sirtuins have also been assayed by monitoring the consumption of NAD^+ or accumulation of the NIC byproduct.[15] These methods work well with recombinant protein systems, but in cell lysates, there are many other enzymes that can change the NAD^+ levels, including the ADP-ribosyltransferases, CD38, and PARP families. Finally, the Cravatt group has used activity-based probes to identify deacetylases in lysates obtained from several cancer cell lines,[12a,b] and the Drewes group has used a chemoproteomic strategy along with KDAC inhibitors for discovering inhibitor−protein binding interactions.[12d] These mass spectrometry-based approaches are powerful for identifying deacetylases and their binding partners in complex lysates, but substantial experimental effort is required to process and analyze samples. The method we present here brings a high-throughput approach for directly monitoring deacetylase activity and does not rely on extraneous enzymatic reagents for detection.

dx.doi.org/10.1021/ac402614x | Anal. Chem. 2013, 85, 10635−10642

Using our peptide arrays, we found that PMA-induced Mk differentiation of CHRF cells is marked by a profound decrease in SIRT activity, while the activity of KDACs 1-11 remains fairly constant. Decreased SIRT deacetylase activity was observed for 324 of 361 substrates, and for these, the average decrease in activity was ~70% (68 ± 23%). We used Western blots to find that SIRTs 1, 2, and 7 protein levels were decreased on day 6 after PMA treatment (Figure 6A), consistent with the decreased SIRT activity. A prominent role for SIRTs 1 and 2 is also consistent with results using the SIRT1/2 inhibitor, EX-527, on lysates obtained from cells prior to PMA-induced differentiation. SIRT5 and SIRT6 levels remained constant after PMA treatment, while interestingly SIRT3 levels increased dramatically. It is well established that protein expression often does not correlate well with enzyme activity. Furthermore, others have demonstrated that post-translational modifications to the SIRTs, as well as their regulatory binding partners, can alter their activity.[16]

The pathways and mechanisms that regulate Mk polyploidization and proplatelet formation (PPF) remain active areas of research. We previously reported that NIC greatly increases the ploidy and PPF of Mk cells derived from $CD34^+$ hematopoietic stem and progenitor cells (HSPCs) in culture.[17] This has been confirmed by the Pineault group[18] and others.[19] Consistent with these results, our current findings suggest that PMA-induced Mk differentiation of CHRF cells may be partially mediated by decreased activity of sirtuins, especially SIRT1 and SIRT2. SIRTs and other KDACs have also been implicated in regulating the expansion and differentiation of HSPCs,[20] as well as in many other cell lineages.[21]

CONCLUSION

This work introduces the use of peptide arrays and SAMDI mass spectrometry to profile enzyme activities in cell lysates. The present work has identified the loss in activity of SIRT1 and SIRT2 during terminal differentiation of the CHRF Mk cell line and illustrates the use of inhibitors to dissect the activity profiles to understand the enzymes that are involved in a change in activities. The use of a label-free analytical method makes this technique readily applicable to a broad range of enzyme activities and provides a new opportunity for identifying changes in global activity profiles that characterize the states of cells.

ASSOCIATED CONTENT

Supporting Information

Additional information and data set. This material is available free of charge via the Internet at http://pubs.acs.org.

AUTHOR INFORMATION

Corresponding Authors

*E-mail: wmmiller@northwestern.edu (W.M.M.).
*E-mail: milan.mrksich@northwestern.edu (M.M.).

Author Contributions

‖H.-Y.K. and T.A.D. contributed equally to this work.

Notes

The authors declare no competing financial interest.

ACKNOWLEDGMENTS

The research was supported by NCI Award U54CA143869 (M.M.), NIH grants GM084188 (M.M.) and HL93083 (W.M.M.), and NSF grant CBET-0853603 (W.M.M.). T.A.D. was supported in part by NIH/NCI training grant T32 CA09560. This work used facilities of the Northwestern University Flow Cytometry Core Facility and a Cancer Center Support Grant (NCI CA060553) and the Northwestern University High Throughput Analysis Lab. We thank Alexei Ten for providing recombinant KDAC8, Courtney Jacqueline Sobers for providing recombinant SIRT3, and Dr. Neda Bagheri for helpful statistics discussions. Any opinions, findings, and conclusions or recommendations expressed in this material are those of the authors and do not necessarily reflect the views of the National Science Foundation.

REFERENCES

(1) (a) Kaeberlein, M.; McDonagh, T.; Heltweg, B.; Hixon, J.; Westman, E. A.; Caldwell, S. D.; Napper, A.; Curtis, R.; DiStefano, P. S.; Fields, S.; Bedalov, A.; Kennedy, B. K. *J. Biol. Chem.* **2005**, *280* (17), 17038−17045. (b) Borra, M. T.; Smith, B. C.; Denu, J. M. *J. Biol. Chem.* **2005**, *280* (17), 17187−17195. (c) Su, J.; Rajapaksha, T. W.; Peter, M. E.; Mrksich, M. *Anal. Chem.* **2006**, *78* (14), 4945−4951.

(2) (a) Frank, R. *J. Immunol. Methods* **2002**, *267* (1), 13−26. (b) Reineke, U.; Volkmer-Engert, R.; Schneider-Mergener, J. *Curr. Opin. Biotechnol.* **2001**, *12* (1), 59−64. (c) Smith, B. C.; Settles, B.; Hallows, W. C.; Craven, M. W.; Denu, J. M. *ACS Chem. Biol.* **2010**, *6* (2), 146−157. (d) Gurard-Levin, Z. A.; Kilian, K. A.; Kim, J.; Bähr, K.; Mrksich, M. *ACS Chem. Biol.* **2010**, *5* (9), 863−873. (e) Rathert, P.; Zhang, X.; Freund, C.; Cheng, X.; Jeltsch, A. *Chem. Biol.* **2008**, *15* (1), 5−11.

(3) (a) Choudhary, C.; Kumar, C.; Gnad, F.; Nielsen, M. L.; Rehman, M.; Walther, T. C.; Olsen, J. V.; Mann, M. *Science* **2009**, *325* (5942), 834−840. (b) Yang, X.-J.; Seto, E. *Mol. Cell* **2008**, *31* (4), 449−461.

(4) Mrksich, M. *ACS Nano* **2008**, *2* (1), 7−18.

(5) Martini, E.; Roche, D. M.; Marheineke, K.; Verreault, A.; Almouzni, G. *J. Cell Biol.* **1998**, *143* (3), 563−575.

(6) Rasband, W. *ImageJ*; National Institutes of Health: Bethesda, Maryland, USA, 1997−2012.

(7) Fuhrken, P. G.; Chen, C.; Miller, W. M.; Papoutsakis, E. T. *Exp. Hematol.* **2007**, *35* (3), 476−489.

(8) Gurard-Levin, Z. A.; Kim, J.; Mrksich, M. *ChemBioChem* **2009**, *10* (13), 2159−2161.

(9) Yoshida, M.; Kijima, M.; Akita, M.; Beppu, T. *J. Biol. Chem.* **1990**, *265* (28), 17174−17179.

(10) Bitterman, K. J.; Anderson, R. M.; Cohen, H. Y.; Latorre-Esteves, M.; Sinclair, D. A. *J. Biol. Chem.* **2002**, *277* (47), 45099−45107.

(11) Peck, B.; Chen, C.-Y.; Ho, K.-K.; Di Fruscia, P.; Myatt, S. S.; Coombes, R. C.; Fuchter, M. J.; Hsiao, C.-D.; Lam, E. W.-F. *Mol. Cancer Ther.* **2010**, *9* (4), 844−855.

(12) (a) Salisbury, C. M.; Cravatt, B. F. *J. Am. Chem. Soc.* **2008**, *130* (7), 2184−2194. (b) Salisbury, C. M.; Cravatt, B. F. *Proc. Natl. Acad. Sci.* **2007**, *104* (4), 1171−1176. (c) Garske, A. L.; Denu, J. M. *Biochemistry* **2005**, *45* (1), 94−101. (d) Bantscheff, M.; Hopf, C.; Savitski, M. M.; Dittmann, A.; Grandi, P.; Michon, A.-M.; Schlegl, J.; Abraham, Y.; Becher, I.; Bergamini, G.; Boesche, M.; Delling, M.; Dumpelfeld, B.; Eberhard, D.; Huthmacher, C.; Mathieson, T.; Poeckel, D.; Reader, V.; Strunk, K.; Sweetman, G.; Kruse, U.; Neubauer, G.; Ramsden, N. G.; Drewes, G. *Nat. Biotechnol.* **2011**, *29* (3), 255−265.

(13) (a) Ban, L.; Pettit, N.; Li, L.; Stuparu, A. D.; Cai, L.; Chen, W.; Guan, W.; Han, W.; Wang, P. G.; Mrksich, M. *Nat. Chem. Biol.* **2012**, *8* (9), 769−773. (b) Gurard-Levin, Z. A.; Scholle, M. D.; Eisenberg, A. H.; Mrksich, M. *ACS Comb. Sci.* **2011**, *13* (4), 347−350.

(14) (a) Bonfils, C.; Kalita, A.; Dubay, M.; Siu, L. L.; Carducci, M. A.; Reid, G.; Martell, R. E.; Besterman, J. M.; Li, Z. *Clin. Cancer Res.* **2008**, *14* (11), 3441−3449. (b) Howitz, K. T.; Bitterman, K. J.; Cohen, H. Y.; Lamming, D. W.; Lavu, S.; Wood, J. G.; Zipkin, R. E.; Chung, P.; Kisielewski, A.; Zhang, L.-L.; Scherer, B.; Sinclair, D. A. *Nature* **2003**, *425* (6954), 191−196.

(15) Smith, B. C.; Hallows, W. C.; Denu, J. M. *Anal. Biochem.* **2009**, *394* (1), 101−109.
(16) (a) Sasaki, T.; Maier, B.; Koclega, K. D.; Chruszcz, M.; Gluba, W.; Stukenberg, P. T.; Minor, W.; Scrable, H. *PLoS One* **2008**, *3* (12), 24. (b) Nasrin, N.; Kaushik, V. K.; Fortier, E.; Wall, D.; Pearson, K. J.; de Cabo, R.; Bordone, L. *PLoS One* **2009**, *4* (12), 0008414. (c) Han, Y.; Jin, Y. H.; Kim, Y. J.; Kang, B. Y.; Choi, H. J.; Kim, D. W.; Yeo, C. Y.; Lee, K. Y. *Biochem. Biophys. Res. Commun.* **2008**, *375* (4), 576−580. (d) Jin, Y. H.; Kim, Y. J.; Kim, D. W.; Baek, K. H.; Kang, B. Y.; Yeo, C. Y.; Lee, K. Y. *Biochem. Biophys. Res. Commun.* **2008**, *368* (3), 690−695.
(17) (a) Giammona, L. M.; Fuhrken, P. G.; Papoutsakis, E. T.; Miller, W. M. *Br. J. Haematol.* **2006**, *135* (4), 554−566. (b) Giammona, L. M.; Panuganti, S.; Kemper, J. M.; Apostolidis, P. A.; Lindsey, S.; Papoutsakis, E. T.; Miller, W. M. *Exp. Hematol.* **2009**, *37* (11), 1340−1352.
(18) Leysi-Derilou, Y.; Duchesne, C.; Garnier, A.; Pineault, N. *Differentiation* **2012**, *83* (4), 200−209.
(19) (a) Avanzi, M. P.; Chen, A.; He, W.; Mitchell, W. B. *Transfusion* **2012**, *52*, 2406−2413. (b) Emmrich, S.; Henke, K.; Hegermann, J.; Ochs, M.; Reinhardt, D.; Klusmann, J. H. *Ann. Hematol.* **2012**, *91* (11), 1673−1684.
(20) (a) Wada, T.; Kikuchi, J.; Nishimura, N.; Shimizu, R.; Kitamura, T.; Furukawa, Y. *J. Biol. Chem.* **2009**, *284* (44), 30673−30683. (b) Peled, T.; Shoham, H.; Aschengrau, D.; Yackoubov, D.; Frei, G.; Rosenheimer, G. N.; Lerrer, B.; Cohen, H. Y.; Nagler, A.; Fibach, E.; Peled, A. *Exp. Hematol.* **2012**, *40* (4), 342−355.
(21) (a) Frumm, S. M.; Fan, Z. P.; Ross, K. N.; Duvall, J. R.; Gupta, S.; Verplank, L.; Suh, B. C.; Holson, E.; Wagner, F. F.; Smith, W. B.; Paranal, R. M.; Bassil, C. F.; Qi, J.; Roti, G.; Kung, A. L.; Bradner, J. E.; Tolliday, N.; Stegmaier, K. *Chem. Biol.* **2013**, *20* (5), 713−725. (b) Xu, S.; De Veirman, K.; Evans, H.; Santini, G. C.; Vande Broek, I.; Leleu, X.; De Becker, A.; Van Camp, B.; Croucher, P.; Vanderkerken, K.; Van Riet, I. *Acta Pharmacol. Sin.* **2013**, *34* (5), 699−709. (c) Conway, G. D.; O'Bara, M. A.; Vedia, B. H.; Pol, S. U.; Sim, F. J. *Glia* **2012**, *60* (12), 1944−1953.